CHEMISTRY & SUSTAINABILITY

CHEMSUSCHEM

ENERGY & MATERIALS

# Accepted Article

**Title:** Mesoporous Carbon Nanospheres Encapsulated Ultrasmall Ir Clusters as Highly Selective Nanocatalysts for (Bio-)Alcohols Methylation Using Methanol as Sustainable C1 Feedstock

**Authors:** Qiang Liu, Guoqiang Xu, Zhendong Wang, Xiaoran Liu, Xicheng Wang, Linlin Dong, Xindong Mu, and Huizhou Liu



**To be cited as:** *ChemSusChem* 10.1002/cssc.201701607

**Link to VoR:** http://dx.doi.org/10.1002/cssc.201701607

A Journal of

ChemPubSoc Europe

WILEY-VCH

www.chemsuschem.org

# Mesoporous Carbon Nanospheres Encapsulated Ultrasmall Ir Clusters as Highly Selective Nanocatalysts for (Bio-)Alcohols Methylation Using Methanol as Sustainable C1 Feedstock

Qiang Liu,[a,b] Guoqiang Xu,*[a] Zhendong Wang,[c] Xiaoran Liu,[a] Xicheng Wang,[a] Linlin Dong,[a] Xindong Mu,*[a] and Huizhou Liu[a]

**Abstract:** C-H methylation is an attractive chemical transformation for C-C bonds construction in organic chemistry, yet efficient methylation of readily available (bio-)alcohols in water using methanol as sustainable C1 feedstock is limited. Herein, yolk-shell-structured mesoporous carbon nanospheres encapsulated Ir nanocatalysts (Ir@YSMCNs) have been synthesized for this transformation. Monodispersed Ir clusters (ca. 1.0 nm) were in situ encapsulated and spatially isolated within YSMCNs by a silica-assisted sol-gel emulsion strategy. A selection of (bio-)alcohols (19 examples) was selectively methylated in aqueous phase with good-to-high yields over the developed Ir@YSMCNs. The improved catalytic efficiencies in terms of activity, selectivity together with the good stability and recyclability were contributable to the ultrasmall Ir clusters with oxidation chemical state as a consequence of the confinement effect of YSMCNs with interconnected nanostructures.

## Introduction

The efficient and selective upgrading of biomass-derived platform compounds for value-added commodity chemicals and transportation biofuels have attracted enormous research interests.[1] (Bio-)alcohols are fundamental chemicals in industries and could also be used as blending stocks for gasoline. However, the intrinsically existent drawbacks in the latter applications including lower energy density and inevitable engine corrosion manifest the high requirement for the efficient upgrading of (bio-)alcohols. Various catalytic approaches such as the Guerbet condensations and α-alkylations process involving C-C bonds formation strategy have been developed up to date.[2] We recently developed the selective upgrading of bio-ethanol and biomass-derived alcohol mixtures (*e.g.*, ethanol-isopropanol-butanol) for the production of advanced biofuels components catalysed by water-tolerant heterogeneous Ir and Pd catalysts.[3] However, efficient transformation routes for the valorization of (bio-)alcohols in water are still under request.

Methylation constitutes a significant form of C-H functionalization for C-C bonds construction in organic synthesis.[4] Methanol, as one of the sustainable C1 feedstock, is known to be alternative methylating reagent[5] in comparison with conventionally utilized methyl halides and organometallic methylating complexes.[6] Hydrogen auto-transfer or "borrowing hydrogen" is, therefore, the most accepted mechanism and with water as the only byproduct.[7] To date, however, the reported C-H methylation reactions using methanol as the methylating reagent and with substrate scope pertaining to ketones,[8] allenes,[9] amines[10] and indoles[11] are mainly catalyzed by homogeneous transition metal catalysts (*e.g.*, Ru, Rh and Ir). Efficient C-H methylation of readily available (bio-)alcohols for the synthesis of methyl functionalized higher alcohols is limited.[3a, 10b, 12] To achieve this purpose, besides, the development of highly active, selective and recyclable heterogeneous catalysts is needed from the sustainable and green chemistry viewpoints.

For advanced heterogeneous catalysis, other than creation of strong bonding interactions between the support and the metal, nanoparticles (NPs) fabrication utilizing nanomaterials with unique physicochemical properties to synthesize core-shell nanocatalysts has been recognized as promising strategy.[13] In this regard, high volume-to-ratio NPs could be spatially isolated and confined within nanostructured shells, bring improved catalytic efficiencies in comparison with that supported on bulk solid matrix.[14] Among various nanomaterials used for the fabrication or encapsulation of metal(oxide) functionalities, carbon nanospheres (CNs) has attracted increasing research interests as a result of their excellent thermal stability and outstanding structural properties, including micro/meso-porosities and high surface areas.[15] Broad catalytic applications arise when CNs-based metal nanocatalysts are involved.[16]

Several protocols have been developed for the synthesis of carbon nanomaterial fabricated metal catalysts, such as traditional wet chemistry, ship-in-a-bottle, hard template and galvanic replacements.[17] Transition metal (*e.g.,* Ru, Rh, Pd, Pt, Ag and Au) core-shell and rattle-type or yolk-shell NPs (average particle size >2 nm) confined within CNs could be obtained thereof.[18] However, these reported approaches need pre-made NPs by additional use of stabilizers, followed by post-fabrication and calcination, which in turn would block active sites and induce distinct activity loss. Besides, owning to the difficulty in

[a] Q. Liu, Dr. G. Xu, Dr. X. Liu, Dr. X. Wang, Dr. L. Dong, Prof. Dr. X. Mu and Prof. Dr. H. Liu
CAS Key Laboratory of Bio-based Materials
Qingdao Institute of Bioenergy and Bioprocess Technology
Chinese Academy of Sciences
Qingdao, 266101 (PR China)
Fax: (+86) 532-80662724
E-mail: muxd@qibebt.ac.cn, xugq@qibebt.ac.cn.
[b] Q. Liu
University of Chinese Academy of Sciences
Beijing, 100049 (PR China)
[c] Z. Wang
Key Laboratory of Marine Chemistry Theory and Technology of Ministry of Education
Ocean University of China
Qingdao, 266100 (PR China)

Supporting information for this article is given via a link at the end of the document.

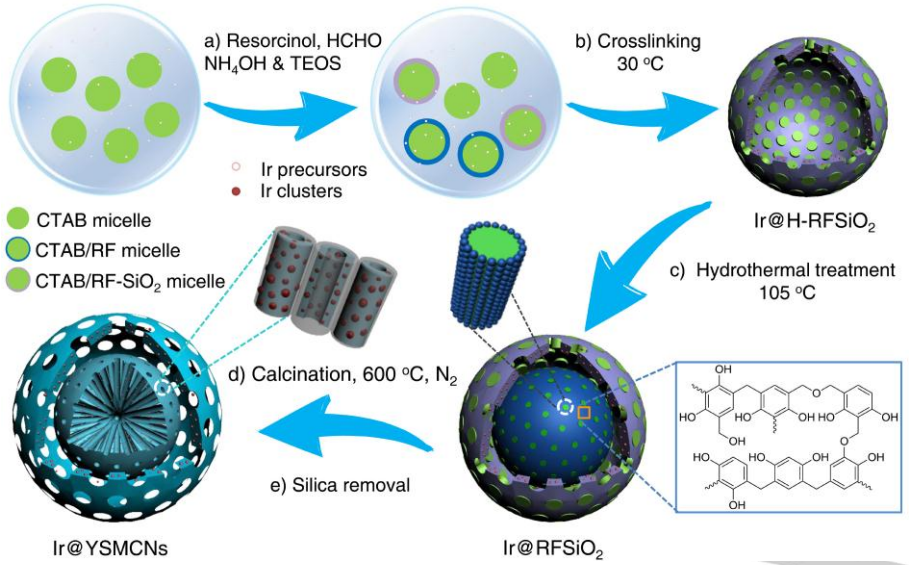


**Scheme 1.** Schematic illustration of synthesis procedure for Ir@YSMCNs.

controlling the NPs migration and overgrowth, limited reports can encapsulate transition metal clusters (<2 nm) within CNs with intrinsically improved activities and stabilities. Hence, unique fabrication nanomaterial is desirable and the in situ encapsulation by directly integrating metal functionalities could be developed to circumvent this challenge.

Herein, we report a silica-assisted sol-gel emulsion strategy for the synthesis of yolk-shell-structured mesoporous carbon nanospheres encapsulated Ir nanocatalysts (Ir@YSMCNs). The developed Ir@YSMCNs feature good functional tolerance, good-to-high yields to methylation products, intrinsically thermal stable and recyclable properties in the selective methylation of a selection of readily available (bio-)alcohols (19 examples) in water using methanol as the sustainable C1 feedstock. The in situ encapsulation strategy for metal clusters fabrication within nanomaterials would open a promising avenue for the synthesis of advanced nanocatalysts with desired catalytic performance.

## Results and Discussion

### Catalyst synthesis and characterizations

The fabrication process of Ir@YSMCNs was based on the recently reported synthetic procedures for hollow-structured CNs with some modifications,[19] and schematically illustrated in Scheme 1. Firstly, Ir precursors (*e.g.,* $IrCl_3$) were directly mixed with cetyltrimethyl ammonium bromide (CTAB, as the cationic templating agent) to achieve the subsequent capture of Ir by efficient interfacial interactions in ethanol-water solutions. Secondly, hollow-structured Ir@H-$RFSiO_2$ nanocomposites with spherical morphologies were formed *via* the sol-gel polymerization and condensation process catalyzed by a base-ammonia after addition of resorcinol/formaldehyde (RF) and tetraethylorthosilicate (TEOS). Then the hydrothermal treatment (HT) process allowed RF species in the presence of CTAB with adsorbed Ir species diffusing into hollowed $RFSiO_2$ nanocomposites. The pre-catalyst Ir@YSMCSiNs was obtained after high-temperature calcination under inert atmosphere. Lastly, the pre-catalyst above underwent silica etching in HF to obtain Ir@YSMCNs(R), where R indicates the water/ethanol volume ratio.

YSMCNs with robust spherical morphologies and encapsulated Ir nanoclusters with high dispersions were obtained by optimizing the synthesis conditions, as characterized by scanning electron microscopy (SEM) and transmission electron microscopy (TEM) images (Figure 1, Figure S2 and S3, Supporting Information). The diameter of Ir@YSMCNs(3.6) is 125±5 nm, and increase with the decreasing of R. Besides, the energy dispersive X-ray (EDX) mapping image and line scanning profile of Ir@YSMCSiNs(3.6) reveal its unique structure: a carbon solid core is surrounded by a hybrid carbon-silica shell (Figure 1c and d), which confirmed the formation of yolk-shell nanostructures after calcination. TEM images of control samples prepared without HT process (Figure S4, Supporting Information) or carbon species removal by air calcination (Figure S5, Supporting Information) further disclose this observation.

As shown in Figure 2b, Ir@YSMCNs(3.6) displays typical IV isotherm curves and H2-type hysteresis loop at $P/P_0$=0.5-1.0,

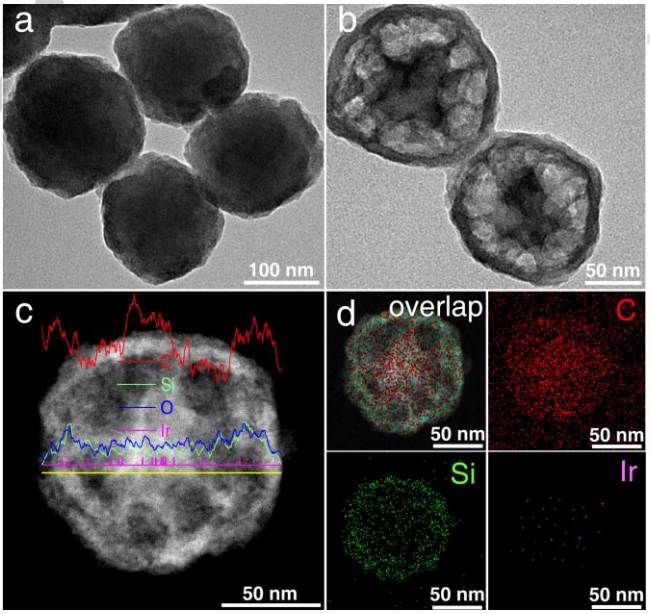


**Figure 1.** TEM images of (a) Ir@$RFSiO_2$(3.6) and (b) Ir@YSMCNs(3.6). (c) Dark-field STEM image of Ir@YSMCSiNs(3.6), inset is the EDX line-scanning profile along the marked line. (d) The EDX mapping images of Ir@YSMCSiNs(3.6) (red: C; green: Si; purple: Ir).

revealing the co-existence of micropores and mesopores with ink-bottle-type morphology. Particularly it has the highest Brunauer-Emmett-Teller (BET) specific surface area (996 $m^2 g^{-1}$) and Barrett-Joyner-Halenda (BJH) pore volume (1.23 $cm^3 g^{-1}$). As further observed, the *t*-plot micropore volume increased with carbon core size (from 0.08 to 0.12 $cm^3 g^{-1}$), suggesting the microporous nature of the inner solid core (Table S1, Supporting Information). All the samples have narrow pore size distributions ranging in 2.6-7.4 nm (Figure S7, Supporting Information), which would not provide diffusion limitations for reactants and products during catalytic reactions. Fourier transform infrared (FT-IR) spectrum in Figure S9 (Supporting Information) demonstrates the complete removal of silica after HF etching procedure. Raman spectroscopy exhibit G-band scattering peaks at 1587 $cm^{-1}$ and D-band at 1358 $cm^{-1}$, revealing that Ir@YSMCNs have graphitization domains (Figure 2c and Table S1, Supporting Information).[20] This observation was further confirmed by powder X-ray diffraction (XRD) analysis (Figure 2d). Two broad diffraction peaks at 22° and 43° are corresponded to the diffraction planes of graphite carbon (002 and 101).[20]

The adsorption and capture of Ir metal ions during synthetic process were analyzed by UV-vis, and demonstrated in Figure S10 in the Supporting Information. CTAB also worked as the stabilizer for Ir clusters formed in the synthesis solutions.[21] High resolution TEM images and XRD patterns, as well as the size distributions of Ir clusters in the synthesized samples are shown in Figure 2a and Figure S11 (Supporting Information). Ir clusters were successfully encapsulated within YSMCNs without detectable clusters or NPs adhering to the exterior surface of YSMCNs. This suggestion is in accordance with the dark field scanning transmission electron microscopy (STEM) image in Figure 1c, where the white spots could be attributed to the monodispersed Ir clusters. The in situ encapsulated Ir clusters have average sizes ranged in 0.9-1.1 nm, which are much smaller than that (3.0 nm) of impregnation-prepared Ir/YSMCNs(3.6)-600 (calcined at 600 °C in $N_2$ for comparison) and that (2.0 nm) of our recently reported Ir/NC (Figure S12, Supporting Information).[3a] In contrast, the Ir NPs migration and aggregate under high temperature were obvious for Ir/YSMCNs(3.6)-600 (Figure S13 and S14, Supporting Information). Besides, CO pulse chemisorption analysis confirmed the higher dispersion (30%) of Ir clusters than that of post-loaded Ir NPs. These findings manifest the advantages of our developed facile in situ encapsulation strategy for the synthesis of ultrasmall metal clusters (*e.g.,* Pd, Ru and Ag) with outstanding sintering resistance properties (Figure S15 and S16, Supporting Information). As mentioned above, the pore size of carbon shell is relatively higher than the cluster size of Ir. The etching of $SiO_2$ contributed to the creation of mesopores in the carbon shell when TEOS was used as hard template for CNs synthesis.[19] Hence, the monodispersed Ir clusters were isolated and encapsulated within the carbon framework.

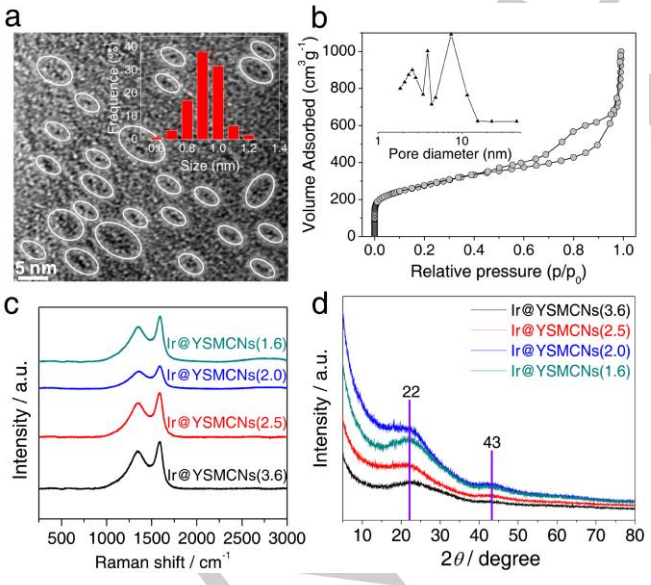


**Figure 2.** (a) HRTEM image of Ir@YSMCNs(3.6). Scale bar: 5 nm. Inset: the Ir cluster size distribution. (b) $N_2$ sorption isotherms of Ir@YSMCNs(3.6). Inset: the pore size distribution. (c) Raman spectroscopy of Ir@YSMCNs prepared with different R. (d) XRD patterns of Ir@YSMCNs (vertical lines show the diffraction peaks of graphitic carbon).

### Catalytic evaluation and substrates scope

The above results suggest the successful synthesis of Ir@YSMCNs containing ultrasmall Ir clusters and mesoporous carbon nanospheres with yolk-shell nanostructures. The methylation of 1-propanol with methanol in water was then selected as the model reaction to explore their catalytic properties. Corresponded catalytic performance of various Ir nanocatalysts are shown in Figure 3 and Table S3 (Supporting Information). To our delight, Ir clusters in situ encapsulated within YSMCNs performed improved catalytic efficiencies in terms of both activity and selectivity in comparison with that of impregnation-prepared Ir/YSMCNs(3.6)-600 and Ir/NC. Notably, Ir@YSMCNs(3.6) gave the highest TOFs (242.3 $h^{-1}$), which was almost 6-fold improvements for Ir/NC (40.5 $h^{-1}$). Moreover, the reaction could still proceed smoothly by using even lower loading of methanol (one equivalent with respect to 1-propanol) (Table S3, entry 8, Supporting Information), which was much

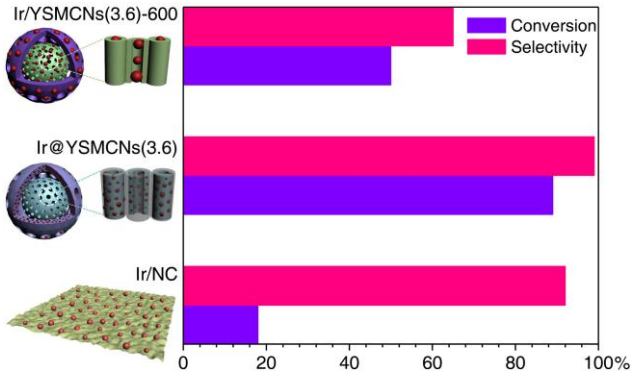


**Figure 3.** Catalytic results of 1-propanol methylation reactions catalyzed by Ir/NC, Ir@YSMCNs(3.6) and Ir/YSMCNs(3.6)-600 under the identical reaction conditions (detail catalytic procedures are presented in Table S3 in the Supporting Information).

**Table 1.** Synthesis of methylated products by selective methylation of (bio-)alcohols with C1 feedstock-methanol in water over Ir@YSMCNs(3.6).[a]

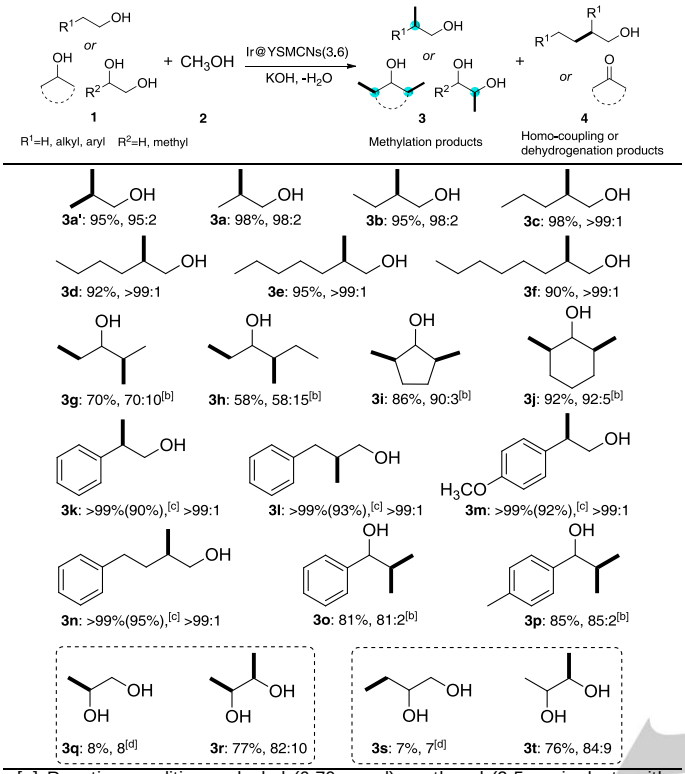


[a] Reaction conditions: alcohol (6.70 mmol), methanol (2-5 equivalents with respect to alcohol), KOH (0.38 g, 6.70 mmol), Ir@YSMCNs(3.6) (0.05 g, 0.076 mol% with respect to alcohol), water (3-5 mL), 170 °C for a certain reaction time (h). Detail methylation conditions of different (bio-)alcohols are summarized in Table S4 in the Supporting Information. GC yields (%) of **3** were based on **1** used. Selectivities (methylation products: homo-coupling products) were determined by GC and GC-MS. [b] Selectivities for di-methylation products: dehydrogenation products. [c] The isolated yields are shown in the corresponding parentheses. [d] The mono-methylated product selectivity.

superior than the reported methylation reactions performed in methanol or other organic solvents.[8-12] This finding reasonably indicates the outstanding ability of Ir nanoclusters for distinguishing the reactivity between methanol and higher alcohols in thermal-basic conditions with water. To the best of our konwledge, besides, such highly efficient methylation reactions in water are first reported involving a large scope of (bio-)alcohols.

The general applicability of this developed methylation protocol catalyzed by Ir@YSMCNs(3.6) was proved by a selection of readily available (bio-)alcohols (Table 1). Aliphatic primary and secondary alcohols, aromatic alcohols, cyclic alcohols (mainly cyclopentanol and cyclohexanol were tested) and diols could all be smoothly featured, resulting in good-to-high yields to methylation products. Methylation reactions of aliphatic linear alcohols (carbon chains ranging in 2-8) proceeded well with up to 90% yield to methylation products, together with almost 100% reactant conversion under the optimized reaction conditions. In the case of secondary and cyclic alcohols, the obtained moderate selectivities to methylation products are possibly related to the higher

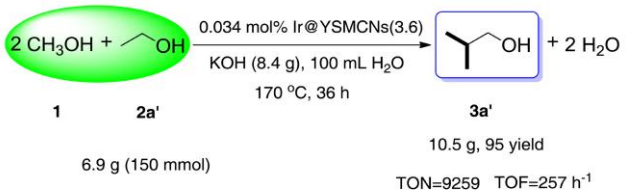


**Scheme 2.** Gram-scale synthesis of iso-butanol by the methylation of ethanol with methanol in water.

dehydrogenation activity or the more than one α-H positions in these alcoholic molecules. Notably, a prolonging of reaction time (>24 h) and elevated reaction temperature (170 °C) were necessary for aromatic alcohols to achieve efficient transformations (Table S4, Supporting Information), possibly owning to their bulky and sterically hindered properties. Besides, diols, such as 1,2-diols could also be selectively methylated to 2,3-diols (76% yield) under moderate reaction conditions. The obtained methylation products, namely the methyl-functionalized higher alcohols are important chemicals and transportation fuel components. In comparison with our early results for iso-butanol synthesis (one of the drop-in biofuels),[3a] the developed Ir nanocatalysts exhibit significant improved activity under moderate reaction conditions. Up to 95% yield of iso-butanol was achieved over Ir@YSMCNs(3.6) at 170 °C using ethanol in water. As a result, notably, the developed methylation process exhibited outstanding practical utility when we performed the gram-scale synthesis of iso-butanol (Scheme 2).

The recyclability and stability of heterogeneous catalysts are important issues for both academic research and industrial applications. The developed Ir nanocatalysts after completion of catalytic methylation reactions were filtrated, washed, and dried directly for the subsequent reuse. Notably, Ir@YSMCNs(3.6) was rather stable to allow several recycling runs without any discernible decrease in selectivity (Figure 4). Although the activity in terms of reactant conversion was slightly decreased after 5 runs, a moderate temperature (200 °C) oxidation

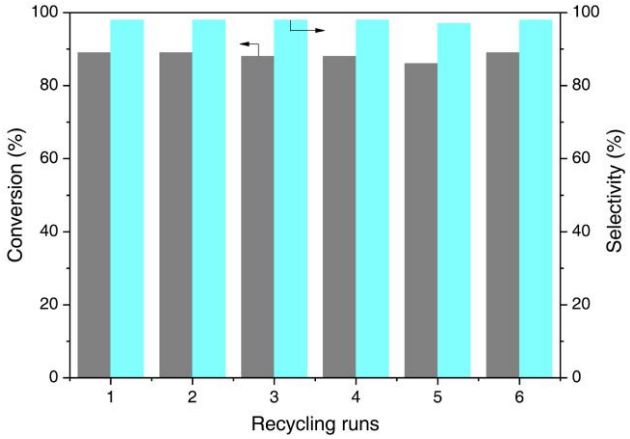


**Figure 4.** The recycling results for the methylation of 1-propanol with methanol under the conditions as that described in Table S3 in the Supporting Information. In the sixth run, the catalytic efficiency was regenerated by 200 °C oxidation of the Ir nanocatalyst filtrated after the fifth reuse.

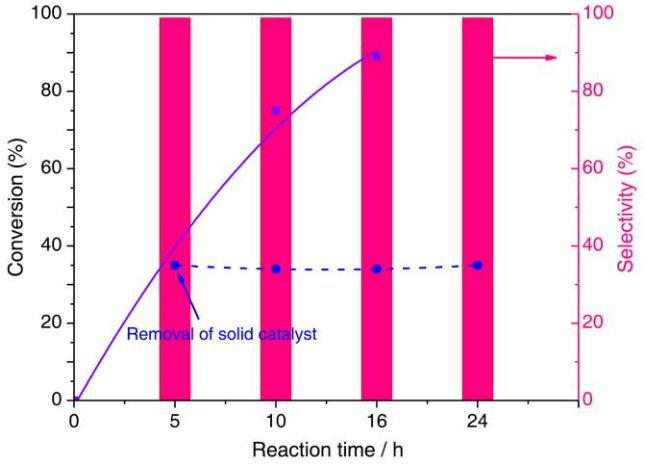


**Figure 5.** (■) The time-resolved experiments for the methylation of 1-propanol with methanol. (●) The hot filtration test for Ir@YSMCNs(3.6) by filtering solid catalyst after temperature cooling down to 100 °C with addition of 13.4 mmol of methanol. The filtrate was allowed to proceed subsequently. Reaction conditions: 1-propanol (0.40 g, 6.70 mmol), methanol (0.43 g, 13.4 mmol), KOH (6.70 mmol), water (5 mL), Ir@YSMCNs(3.6) (0.05 g, 0.076 mol% with respect to 1-propanol), 150 °C, 16h.

procedure could regenerate its catalytic efficiencies. A hot-filtration experiment was then performed (Figure 5). The removal of Ir nanocatalysts after 5 h (*i.e.*, after 35% alcohol conversion) led to the complete termination of methylation reactions, effectively demonstrating the heterogeneous nature of Ir nanocatalysts and ruling out the homogeneous contributions of Ir. The Ir leaching content in the solution was negligible (0.0020 μg $mL^{-1}$, 0.001 wt% with respect to total encapsulated Ir species) suggested by inductively coupled plasma-mass spectrometry (ICP-MS). In comparison, Ir/YSMCNs(3.6)-600 exhibited severe Ir leaching (almost 60 times higher than Ir@YSMCNs(3.6)) after a catalytic recycling. Furthermore, corresponding XRD, TEM and XPS characterizations after catalyst recycling and/or calcination treatment all demonstrated the robust properties of Ir@YSMCNs(3.6) (Figure S17 and S18, Supporting Information). In view of the remarkable advantages of the encapsulated Ir nanoclusters, we believe, the developed in situ encapsulation strategy could be extended to precise design and synthesis other advanced nanocatalysts for broad applications including selective (de)hydrogenations,[16a, 22] coupling reactions.[23]

### Origins of improved catalytic efficiencies

To evaluate origin of the superior activity/selectivity over Ir@YSMCNs(3.6), extensive characterizations and control experiments were conducted. As shown in Figure 6a and Figure S19 (Supporting Information), Ir 4f X-ray photoelectron spectroscopy (XPS) exhibit two doublet peaks with binding energies (BEs) of 62.2 eV (Ir $4f_{7/2}$) and 65.0 eV (Ir $4f_{5/2}$). The peaks around 61.3 eV and 64.2 eV are assigned to $Ir^0$,[24] which are higher than Ir metal due to the formation of Ir

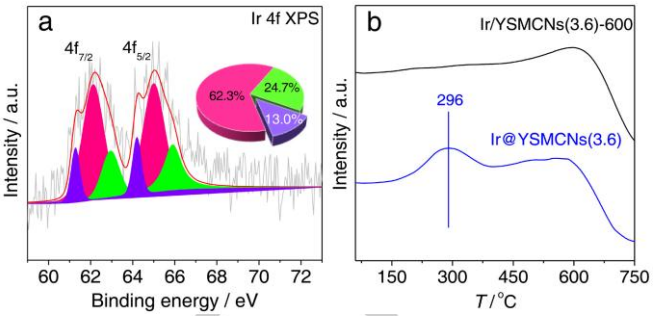


**Figure 6.** (a) XPS spectrum of Ir@YSMCNs(3.6). Inset is the atomic content distribution of $Ir^0$ (purple) and $Ir^{n+}$ (red and green). (b) $H_2$-TPR profiles of Ir@YSMCNs(3.6) and Ir/YSMCNs(3.6)-600.

clusters.Therefore, the peaks centered at higher BEs (*e.g.*, 62.1 eV, 63.0 eV in Ir $4f_{7/2}$) are $IrO_x$ species.[3a, 24] Moreover, Ir@YSMCNs(3.6) has the highest proportion of $Ir^{n+}$ (mainly 87%) that is, $IrO_x$ clusters were partially reduced during high-temperature calcination. This observation was further confirmed by $H_2$ temperature-programmed reduction ($H_2$-TPR) profile of Ir@YSMCNs(3.6) with single broad peak at 296 °C ascribed to the reduction of $IrO_x$ (Figure 6b).[25] However, no reduction peak for Ir/YSMCNs(3.6)-600 was observed, which indicates the largely existent $Ir^0$. Besides, Ir@YSMCNs(3.6) displayed approximately 0.45 eV of BE higher shift than Ir/YSMCNs(3.6)-600, revealing the strong metal-support interactions (SMSIs) in the nanostructures of YSMCNs (Figure S20, Supporting Information). The in situ formed $IrO_x$ clusters were then attributable to the SMSIs by encapsulation within YSMCNs.

While the Ir nanocatalyst prepared by re-oxidization of Ir/YSMCNs(3.6)-600 at 200 °C in air exhibited a 10% conversion increase (Table S3, entry 15, Supporting Information), suggesting the sensitivity of $IrO_x$ for the improved methylation activity. The above result is in accordance with the early report of oxidized Au for alcohols dehydrogenation.[26] Moreover, this suggestion reasonably indicates that ultrasmall Ir cluster size are responsible for the observed extraordinary selectivity for methylation products. Another comparative experiment using Ir/YSMCNs(3.6)-600 with larger Ir NPs (3.0 nm, Table S3, entry 6, Supporting Information) has proved this hypothesis.

In order to gain an in-depth understanding of the methylation reactions, the temperature-programmed desorption-mass spectrum (TPD-MS) analysis was then performed using Ir@YSMCNs(3.6) and Ir/YSMCNs(3.6)-600 for comparative purpose (Figure S21, Supporting Information). When the mole ratio of methanol/1-propanol was fixed as 1/1, the MS signal intensities of formaldehyde and propaldehyde were orders of magnitude higher than that of reactive product intermediates (*e.g.,* unsaturated aldehydes or alcohols), indicating the dehydrogenation of alcohols is not the rate-determining step. This finding could be interpreted by the rapidly increased signals of $H_2$ species when the reaction was eased under continuous $N_2$ flow. Furthermore, $IrO_x$ clusters on Ir@YSMCNs(3.6) displayed a high activity for methanol selective adsorption and activation, as revealed by more intensive MS signals of formaldehyde than

propaldehyde. In contrast, 1-propanol sorptive-dehydrogenation followed by aldol-condensations were facilitated over larger Ir NPs on Ir/YSMCNs(3.6)-600, resulting in poor selectivities to methylation products. Taken together, we propose a plausible methylation pathway in Scheme S1 (Supporting Information). These observations further demonstrate the improved catalytic performance of $IrO_x$ clusters is consequent on the confinement effect of YSMCNs with interconnected nanostructures.

## Conclusions

In summary, a facile strategy was developed for the in situ encapsulation of Ir clusters within yolk-shell-structured mesoporous carbon nanospheres. Monodispersed Ir clusters with high oxidation chemical state exhibited excellent catalytic efficiencies, outstanding recyclability and stability for the selective methylation of readily available (bio-)alcohols in water using methanol as the sustainable C1 feedstock. Moreover, by intensive characterizations and control experiments, the sensitivity of $IrO_x$ nanoclusters for the improved activity and selectivity in the developed (bio-)alcohols methylation reactions was proposed.

## Experimental Section

### Catalyst preparation

In a typical synthesis of Ir@YSMCNs(3.6), 0.010 g of $IrCl_3{\cdot}xH_2O$ was initially dissolved in 10.0 mL of distilled water at 60 $^oC$ to get a clear light-yellow solution. Another solution containing 1.20 g of CTAB, 13.0 mL of absolute ethanol and 37.0 mL of distilled water was added into the Ir solution. After stirring for 30 min, 0.40 g of resorcinol and 0.40 mL of $NH_3{\cdot}H_2O$ were added successively into the resultant solution under vigorous stirring to allow a complete dissolution. Further addition of 0.56 mL of formaldehyde made the brunet transparent solution change to cloudy emulsion. After 20 min, 1.0 mL of TEOS was slowly added to the dispersion and the stirring was continued for 30 h at 25 $^oC$, followed by heating at 105 $^oC$ for another 24 h under a static condition in a Teflon-lined autoclave. Approximately 1.20 g of resultant brown solid product (Ir@RFS$iO_2$(3.6)) was centrifuged, purified by water/ethanol mixture three times and air-dried at 70 $^oC$ for 12 h. Then the yolk-shell carbon-silica composites encapsulated Ir product (Ir@YSMCSiNs(3.6)) was obtained by calcination under $N_2$ atmosphere in a tube furnace: firstly heating to 350 $^oC$ from room temperature at a ramp of 1 $^oC\ min^{-1}$, and kept for 2 h, then heating at a ramp of 1 $^oC\ min^{-1}$ to 600 $^oC$ and kept for another 2 h. After immersing in aqueous HF solution (20.0 mL, 10 wt%) to remove silica at room temperature for 12 h, followed by filtration, washing by distilled water and air-drying at 105 $^oC$, 0.30 g of Ir nanocatalyst, denoted as Ir@YSMCNs(3.6), was finally obtained.

Ir/YSMCNs(3.6)-600 was prepared by conventional wet impregnation method using YSMCNs(3.6) as the support. Typically, 0.010 g of $IrCl_3{\cdot}xH_2O$ was absolutely dissolved in 10.0 mL of distilled water by heating at 60 $^oC$ under stirring. After that, 0.30 g of YSMCNs(3.6) was added and stirred vigorously for 12 h at room temperature. The resultant mixture was evaporated under vacuum to remove the solvent, and then dried at 105 $^oC$ overnight. Finally, the as-synthesized catalyst was calcined at 600 $^oC$ under $N_2$ atmosphere for 2 h to obtain the impregnation-prepared Ir nanocatalyst. The YSMCNs(3.6) support was prepared by using the same silica-assisted sol-gel emulsion procedure as that for Ir@YSMCNs(3.6) without adding of Ir precursors. Ir/NC was prepared according to our very recently reported procedure with slight modifications,[3a] and corresponding preparation details are presented in the Supporting Information.

### Catalyst characterization

Scanning electron microscopy (SEM) images were taken on Hitachi S-4800 with an accelerating voltage of 10.0 kV. Transmission electron microscopy (TEM) and high-resolution transmission electron microscopy (HRTEM) were conducted on Hitachi H-7650 and FEI Tecnai G20 electron microscope, operating at 120 kV and 200 kV, respectively. Dark-field scanning transmission electron microscope (DF-STEM) and the elemental distribution identifications were obtained using energy dispersive X-ray (EDX) spectrometer system equipped on Tecnai G2 F20 S-TWIN. Powder X-ray diffraction (XRD) was performed on Bruker D8 advance equipped with Cu Kα radiation in the scanning range ($2\theta$) of 20-80$^o$. X-ray photoelectron spectroscopy (XPS) was carried out on Thermo Escalab 250XI with Al Kα (1486.6 eV) source. C1s peak with binding energy at 284.8 eV was used as the reference for calibration. Fitting of the Ir 4f spectrum was performed by using two spin-orbit split Ir $4f_{7/2}$ and Ir $4f_{5/2}$ components, which were separated by 2.9 eV with a fixed area ratio of 4/3. $N_2$ adsorption-desorption isotherms were measured at 77 K on Micromeritics ASAP 2020. Brunauer-Emmett-Teller (BET) method and Barret–Joyner–Halenda (BJH) model were used to calculate the specific surface areas and pore size distributions, respectively. The micropore volumes were calculated based on the *t*-plot analysis mode. The temperature-programmed desorption-mass spectrum (TPD-MS) analysis was conducted on Micromeritics AutoChem II 2920 instrument coupled with a mass spectrum analyzer (QIC-20, HIDEN analytical). The reactants (both physically and chemically adsorbed on the sample), products and possible reactive intermediates formed during the reaction were detected on coupled MS unit by RGA bar mode at 70 V electron energy with 1000 ms of mode-change-delay. Ultraviolet visible spectrometry (UV-vis) analyses were performed on Perkin-Elmer Lambda 25 spectrometer with the wavelength ranged in 200 to 800 nm. Fourier transform infrared spectroscopy (FT-IR) was collected on Thermo Scientific Nicolet iN 10 IR Microscope. The samples were scanned 32 times from 400 to 4000 $cm^{-1}$ with a resolution of 4 $cm^{-1}$. Each sample was tableted with KBr prior to each data collection. Raman spectroscopy was detected on Thermo Scientific DXR Microscope. Thermogravimetric (TG) analysis was performed on TA Q600 in Ar atmosphere with a heating rate of 5 $^oC\ min^{-1}$ from 25 to 800 $^oC$. The inductively coupled plasma-mass spectrometry (ICP-MS) was conducted on an Agilent 7700ce instrument.

### Typical methylation procedures and products analysis

In a typical methylation reaction, 0.40 g of 1-propanol (6.70 mmol) and 0.43 g of methanol (13.4 mmol) were mixed with 5.0 mL of distilled water in an autoclave, to which 0.05 g of Ir@YSMCNs(3.6) and 0.38 g of KOH (6.70 mmol, one equivalent with respect to 1-propanol) were added without purging of air. Then the autoclave was heated in oil bath at 150 $^oC$ for 16 h under vigorous stirring. After cooling down to room temperature, the solution was diluted using methanol and then quantified by gas chromatography (GC, Shimadzu 2010 plus, flame ionization detector) equipped with a Rtx-Wax column (30 m × 0.25 μm × 0.32 mm) using anisole as the internal standard. Gas chromatography-mass spectrometry (GC-MS, Shimadzu QP-2010 Ultra) was used to identify the products after each reaction.

## Acknowledgements

We thank the National Natural Science Foundation of China (21273260, 201403265 and 21433001), the Shandong Provincial Natural Science Foundation for Distinguished Young Scholar (JQ201305), The Taishan Scholars Climbing Program of Shandong (tspd20150210), The Young Taishan Scholars Program of Shandong Province (tsqn20161052) and Youth Innovation Promotion Association CAS (2015168) for financial support.

**Keywords:** alcohols• iridium • mesoporous carbon nanospheres • metal clusters • methylation

[1] a) J. Q. Bond, D. M. Alonso, D. Wang, R. M. West, J. A. Dumesic, *Science* **2010**, *327*, 1110-1114; b) B. L. Wegenhart, L. Yang, S. C. Kwan, R. Harris, H. I. Kenttämaa, M. M. Abu-Omar, *ChemSusChem* **2014**, *7*, 2742-2747; c) E. R. Sacia, M. Balakrishnan, M. H. Deaner, K. A. Goulas, F. D. Toste, A. T. Bell, *ChemSusChem* **2015**, *8*, 1726-1736; d) S. Sankaranarayanapillai, S. Sreekumar, J. Gomes, A. Grippo, G. E. Arab, M. Head-Gordon, F. D. Toste, A. T. Bell, *Angew. Chem. Int. Ed.* **2015**, *54*, 4673-4677; *Angew. Chem.* **2015**, *127*, 4756-4760.

[2] a) J. Sun, K. Zhu, F. Gao, C. Wang, J. Liu, C. H. F. Peden, Y. Wang, *J. Am. Chem. Soc.* **2011**, *133*, 11096-11099; b) P. Anbarasan, Z. C. Baer, S. Sreekumar, E. Gross, J. B. Binder, H. W. Blanch, D. S. Clark, F. D. Toste, *Nature* **2012**, *491*, 235-239; c) S. Sreekumar, Z. C. Baer, E. Gross, S. Padmanaban, K. Goulas, G. Gunbas, S. Alayoglu, H. W. Blanch, D. S. Clark, F. D. Toste, *ChemSusChem* **2014**, *7*, 2445-2448; d) G. Xu, Q. Li, J. Feng, Q. Liu, Z. Zhang, X. Wang, X. Zhang, X. Mu, *ChemSusChem* **2014**, *7*, 105-109; e) S. Chakraborty, P. E. Piszel, C. E. Hayes, R. T. Baker, W. D. Jones, *J. Am. Chem. Soc.* **2015**, *137*, 14264-14267; f) H. Aitchison, R. L. Wingad, D. F. Wass, *ACS Catal.* **2016**, *6*, 7125-7132; g) Y. Xie, Y. Ben-David, L. J. W. Shimon, D. Milstein, *J. Am. Chem. Soc.* **2016**, *138*, 9077-9080; h) K.-N. T. Tseng, S. Lin, J. W. Kampf, N. K. Szymczak, *Chem. Commun.* **2016**, *52*, 2901-2904; i) J. Pang, M. Zheng, L. He, L. Li, X. Pan, A. Wang, X. Wang, T. Zhang, *J. Catal.* **2016**, *344*, 184-193.

[3] a) Q. Liu, G. Xu, X. Wang, X. Mu, *Green Chem.* **2016**, *18*, 2811-2818; b) Q. Liu, G. Xu, X. Wang, X. Liu, X. Mu, *ChemSusChem* **2016**, *9*, 3465-3472.

[4] E. J. Barreiro, A. E. Kümmerle, C. A. M. Fraga, *Chem. Rev.* **2011**, *111*, 5215-5246.

[5] a) M. Selva, A. Perosa, *Green Chem.* **2008**, *10*, 457-464; b) K. Natte, H. Neumann, M. Beller, R. V. Jagadeesh, *Angew. Chem. Int. Ed.* **2017**, *56*, 6384-6394; *Angew. Chem.* **2017**, *129*, 6482-6492.

[6] a) D. Shabashov, O. Daugulis, *J. Am. Chem. Soc.* **2010**, *132*, 3965-3972; b) S.-Y. Zhang, G. He, W. A. Nack, Y. Zhao, Q. Li, G. Chen, *J. Am. Chem. Soc.* **2013**, *135*, 2124-2127; c) R. Shang, L. Ilies, E. Nakamura, *J. Am. Chem. Soc.* **2015**, *137*, 7660-7663; d) X. Chen, J.-J. Li, X.-S. Hao, C. E. Goodhue, J.-Q. Yu, *J. Am. Chem. Soc.* **2006**, *128*, 78-79; e) Q. Chen, L. Ilies, N. Yoshikai, E. Nakamura, *Org. Lett.* **2011**, *13*, 3232-3234.

[7] M. H. S. A. Hamid, P. A. Slatford, J. M. J. Williams, *Adv. Synth. Catal.* **2007**, *349*, 1555-1575.

[8] a) S. Ogawa, Y. Obora, *Chem. Commun.* **2014**, *50*, 2491-2493; b) L. K. M. Chan, D. L. Poole, D. Shen, M. P. Healy, T. J. Donohoe, *Angew. Chem. Int. Ed.* **2014**, *53*, 761-765; *Angew. Chem.* **2014**, *126*, 780-784; c) X. Quan, S. Kerdphon, P. G. Andersson, *Chem. Eur. J.* **2015**, *21*, 3576-3579; d) T. T. Dang, A. M. Seayad, *Adv. Synth. Catal.* **2016**, *358*, 3373-3380.

[9] J. Moran, A. Preetz, R. A. Mesch, M. J. Krische, *Nat. Chem.* **2011**, *3*, 287-290.

[10] a) T. T. Dang, B. Ramalingam, A. M. Seayad, *ACS Catal.* **2015**, *5*, 4082-4088; b) K. Oikawa, S. Itoh, H. Yano, H. Kawasaki Y. Obora, *Chem. Commun.* **2017**, *53*, 1080-1083; c) A. Bruneau-Voisine, D. Wang, V. Dorcet, T. Roisnel, C. Darcel, J.-B. Sortais, *J. Catal.* **2017**, *347*, 57-62.

[11] S.-J. Chen, G.-P. Lu, C. Cai, *RSC Adv.* **2015**, *5*, 70329-70332.

[12] Y. Li, H. Li, H. Junge, M. Beller, *Chem. Commun.* **2014**, *50*, 14991-14994.

[13] a) J. Sun, X. Bao, *Chem. Eur. J.* **2008**, *14*, 7478-7488; b) P. Hu, J. V. Morabito, C.-K. Tsung, *ACS Catal.* **2014**, *4*, 4409-4419; c) G. Prieto, H. Tüysüz, N. Duyckaerts, J. Knossalla, G.-H. Wang, F. Schüth, *Chem. Rev.* **2016**, *116*, 14056-14119.

[14] H. Yang, S. J. Bradley, A. Chan, G. I. N. Waterhouse, T. Nann, P. E. Kruger, S. G. Telfer, *J. Am. Chem. Soc.* **2016**, *138*, 11872-11881.

[15] a) R. J. White, K. Tauer, M. Antonietti, M.-M. Titirici, *J. Am. Chem. Soc.* **2010**, *132*, 17360-17363; b) J. Liu, S. Z. Qiao, H. Liu, J. Chen, A. Orpe, D. Zhao, G. Q. Lu, *Angew. Chem. Int. Ed.* **2011**, *50*, 5947-5951; *Angew. Chem.* **2011**, *123*, 6069-6073; c) R. Liu, S. M. Mahurin, C. Li, R. R. Unocic, J. C. Idrobo, H. Gao, S. J. Pennycook, S. Dai, *Angew. Chem. Int. Ed.* **2011**, *50*, 6799-6802; *Angew. Chem.* **2011**, *123*, 6931-6934.

[16] a) S. Ikeda, S. Ishino, T. Harada, N. Okamoto, T. Sakata, H. Mori, S. Kuwabata, T. Torimoto, M. Matsumura, *Angew. Chem. Int. Ed.* **2006**, *45*, 7063-7066; *Angew. Chem.* **2006**, *118*, 7221-7224; b) G.-H. Wang, J Hilgert, F. H. Richter, F. Wang, H.-J. Bongard, B. Spliethoff, C. Weidenthaler, F. Schüth, *Nat. Mater.* **2014**, *13*, 293-300; c) G.-H. Wang Z. Cao, D. Gu, N. Pfander, A.-C. Swertz, B. Spliethoff, H.-J. Bongard, C Weidenthaler, W. Schmidt, R. Rinaldi, F. Schüth, *Angew. Chem. Int. Ed* **2016**, *55*, 8850-8855; *Angew. Chem.* **2016**, *128*, 8996-9001.

[17] J. Liu, S. Z. Qiao, J. S. Chen, X. W. Lou, X. Xing, G. Q. Lu, *Chem. Commun.* **2011**, *47*, 12578-12591.

[18] a) R. Liu, F. Qu, Y. Guo, N. Yao, R. D. Priestley, *Chem. Commun.* **2014**, *50*, 478-480; b) T. Harada, S. Ikeda, Y. H. Ng, T. Sakata, H. Mori, T. Torimoto, M. Matsumura, *Adv. Funct. Mater.* **2008**, *18*, 2190-2196; c) T. Yang, J. Liu, Y. Zheng, M. J. Monteiro, S. Z. Qiao, *Chem. Eur. J.* **2013**, *19*, 6942-6945; d) H. Liu, Z. Feng, J. Wang, L. Zhang, D. S. Su, *Catal. Today* **2016**, *260*, 55-59; e) T. N. Phaahlamohlaka, D. O. Kumi, M. W. Dlamini, L. L. Jewell, N. J. Coville, *Catal. Today* **2016**, *275*, 76-83.

[19] J. Hou, T. Cao, F. Idrees, C. Cao, *Nanoscale* **2016**, *8*, 451-457.

[20] C. Li, Y. Meng, S. Wang, M. Qian, J. Wang, W. Lu, R. Huang, *ACS Nano* **2015**, *9*, 12096-12103.

[21] J. Chen, R. Zhang, L. Han, B. Tu, D. Zhao, *Nano Res.* **2013**, *6*, 871-879.

[22] a) Z.-A. Qiao, P. Zhang, S.-H. Chai, M. Chi, G. M. Veith, N. C. Gallego, M. Kidder, S. Dai, *J. Am. Chem. Soc.* **2014**, *136*, 11260-11263; b) C. Wang, L. Wang, J. Zhang, H. Wang, J. P. Lewis, F.-S. Xiao, *J. Am. Chem. Soc.* **2016**, *138*, 7880-7883.

[23] T.-L. Cui, W.-Y. Ke, W.-B. Zhang, H.-H. Wang, X.-H. Li, J.-S. Chen, *Angew. Chem. Int. Ed.* **2016**, *55*, 9178-9182; *Angew. Chem.* **2016**, *128*, 9324-9328.

[24] J. Wang, D. Ge, X. Cao, M. Tang, Y. Pan, H. Gu, *Chem. Commun.* **2015**, *51*, 9216-9219.

[25] Q.-Y. Bi, J.-D. Lin, Y.-M. Liu, S.-H. Xie, H.-Y. He, Y. Cao, *Chem. Commun.* **2014**, *50*, 9138-9140.

[26] A. Wittstock, V. Zielasek, J. Biener, C. M. Friend, M. Bäumer, *Science* **2010**, *327*, 319-322.

# FULL PAPER

Methylation, one of the fundamental C-H functionalization reactions for C-C bonds construction, is developed as efficient approach for the direct upgrading of (bio-)alcohols in pure water. A selection of (bio-)alcohols is highly selective methylated using methanol as a sustainable C1 feedstock over ultrasmall iridium clusters in situ encapsulated within mesoporous carbon nanospheres with yolk-shell nanostructures.

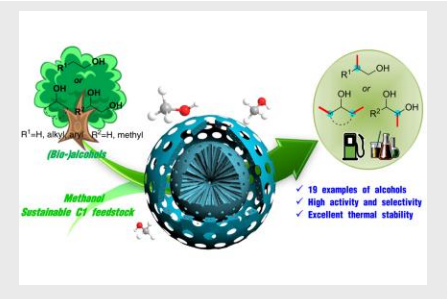


*Q. Liu, G. Xu,* Z. Wang, X. Liu, X. Wang, L. Dong, X. Mu,* and H. Liu*

***Page No. – Page No.***

**Mesoporous Carbon Nanospheres Encapsulated Ultrasmall Ir Clusters as Highly Selective Nanocatalysts for (Bio-)Alcohols Methylation Using Methanol as Sustainable C1 Feedstock**